nature biotechnology

REVIEW ARTICLE

https://doi.org/10.1038/s41587-019-0341-6

Probing and engineering liquid-phase organelles

Dan Bracha[1,3], Mackenzie T. Walls[1,3] and Clifford P. Brangwynne[1,2*]

Cells compartmentalize their intracellular environment to orchestrate countless simultaneous biochemical processes. Many intracellular tasks rely on membrane-less organelles, multicomponent condensates that assemble by liquid–liquid phase separation. A decade of intensive research has provided a basic understanding of the biomolecular driving forces underlying the form and function of such organelles. Here we review the technologies enabling these developments, along with approaches to designing spatiotemporally actuated organelles based on multivalent low-affinity interactions. With these recent advances, it is now becoming possible both to modulate the properties of native condensates and to engineer entirely new structures, with the potential for widespread biomedical and biotechnological applications.

A central feature of biological systems is compartmentalization across diverse length scales—from organs to submicron intracellular organelles. Just as tissue-engineered organs hold great promise for human health, efforts toward reprograming, mending or creating intracellular compartments through organelle engineering have the potential to fundamentally change our ability to modulate physiological processes. The best-known organelles are membrane-bound structures, but cells also contain many organelles without membranes that have diverse biological functions. However, until recently, both the principles underlying the assembly of membrane-less organelles and their biophysical properties have been largely unknown, hindering our ability to rationally design and exploit them for biotechnological purposes.

Over the last decade, our understanding of these structures has advanced rapidly, beginning with the discovery that membrane-less organelles known as P granules assemble through the condensation of various proteins and RNAs into liquid droplets[1]. This process, known as liquid–liquid phase separation (LLPS), has since been implicated in the assembly of dozens of membrane-less structures, increasingly referred to as condensates, where it plays a central role in the diverse structural and functional properties they exhibit (Fig. 1)[2,3]. For instance, coalescence of nucleoli[4], reversible assembly and biomolecule sequestration of stress granules[5] and genome organization by enhancer clusters and heterochromatin[6–10] are all thought to arise from LLPS, which yields malleable and dynamic liquid-like structures that facilitate various biological functions. However, native condensates are far from simple liquids; mixed biomolecular interaction modes and rich compositional heterogeneity within the nonequilibrium intracellular environment yield complex viscoelastic structures, which can be spatially patterned and multilayered and can exhibit nonuniform material properties (Fig. 1).

The development of biomedical and biotechnological applications based on these fundamental advances requires a detailed understanding of the molecular and biophysical principles underlying condensate assembly. We know from nonliving polymeric and soft-matter systems that a key requirement for constituent molecules to undergo phase separation is the presence of multiple interaction segments capable of forming low-affinity interactions[11–14]. This feature, referred to as multivalency, enables interactions with multiple partners, thereby creating a network of dynamically rearranging crosslinks among the component molecules.

Valence can be modulated through various post-translational modifications, including the regulation of homo- and hetero-oligomerization domains. Apart from linking together multiple folded interaction domains, evolution has yielded a more compact means for multivalency through the use of self-associating intrinsically disordered protein regions (IDRs). These IDRs act as 'sticky' biopolymers via short patches of interacting residues patterned along their unstructured chain, which collectively promote LLPS. Despite this increased understanding, key challenges remain in elucidating the functional internal architecture that emerges from these underlying molecular driving forces.

Much of the work in this field has relied on in vitro reconstitution, or overexpression of proteins in living cells to examine their capacity to condense into dynamic puncta. However, a growing suite of new technologies is advancing our understanding of the biophysical principles underlying intracellular phase separation, including the role of the spectrum of condensate states—from liquid droplets to more viscoelastic, solid-like hydrogels—in biological function and dysfunction. Here, we discuss the development and application of these state-of-the-art technologies. We begin by examining technologies being used to develop a quantitative and rigorous understanding of the structure–function relationships in native biological condensates and then discuss how these technologies and insights can be harnessed for novel bioengineering applications.

Probing the properties of phase-separated organelles

Several technologies are enabling elucidation of the precise composition of biomolecular condensates and interrogation of the material properties and associated molecular transport dynamics within. These are discussed in more detail below.

Composition, structure and dynamics. The composition of many condensates has been arrived at piecemeal over the past several decades through conventional molecular biology approaches, such as antibody staining, mass spectrometry analysis and fluorescent protein colocalization studies. However, many condensates appear particularly labile and are therefore not well suited for intact purification[15], requiring different approaches to study their properties and the functional consequences in situ.

This challenge is being addressed by proximity-labeling approaches, such as proximity-dependent biotin identification

[1]Department of Chemical and Biological Engineering, Princeton University, Princeton, NJ, USA. [2]Howard Hughes Medical Institute, Department of Chemical and Biological Engineering, Princeton University, Princeton, NJ, USA. [3]These authors contributed equally: Dan Bracha, Mackenzie T. Walls. *e-mail: cbrangwy@princeton.edu

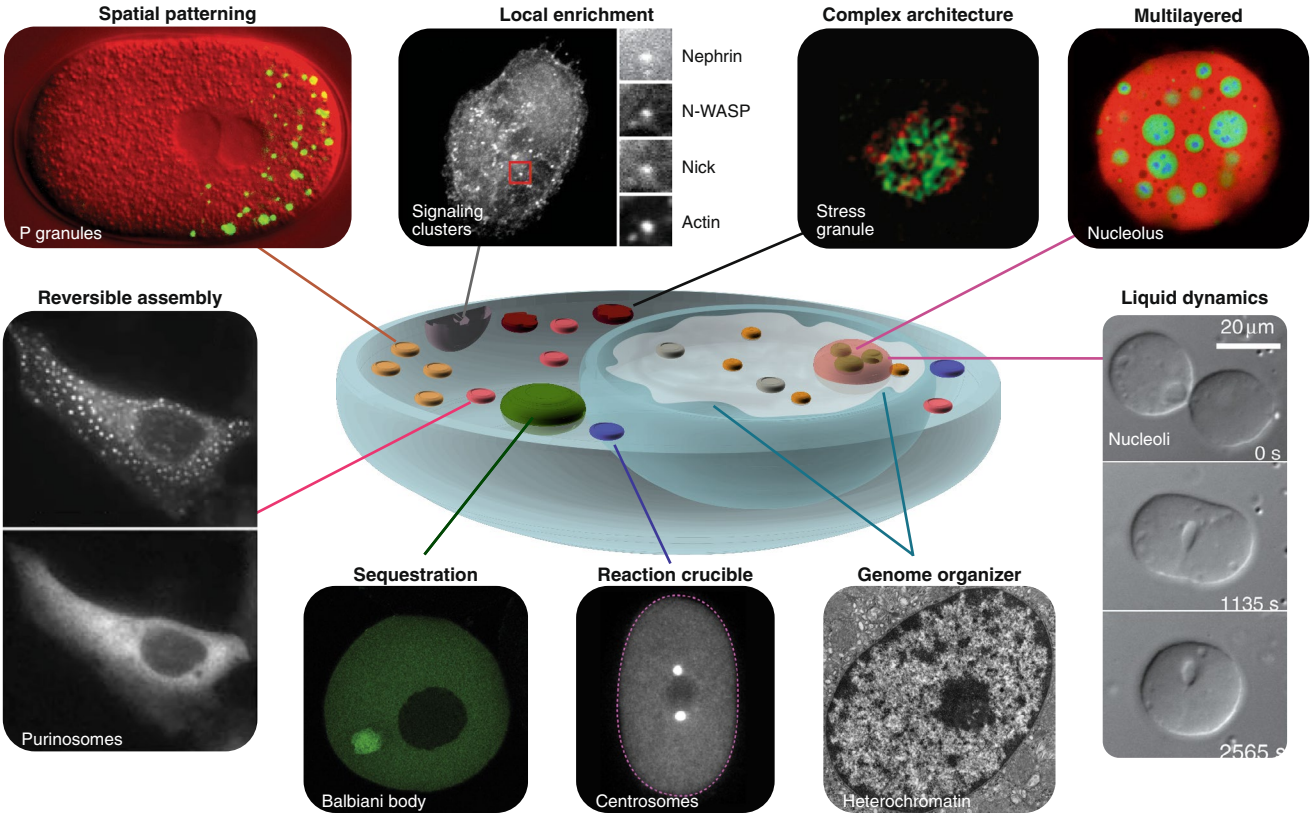

Fig. 1 | Diversity of condensate forms and functions in living cells. Condensates within living cells have unique features that directly inform their function. Images adapted with permission from AAAS[1,98,105], Elsevier[47,100,106], PNAS[48], Mateju et al.[107] and H. Jastrow[108].

(BioID) and labeling via ascorbate peroxidase (Apex)[16,17], that can reveal dynamic networks of interactions; in such approaches, known condensate-enriched proteins are tagged with an enzyme that biotinylates adjacent proteins, which can then be purified with streptavidin-based precipitation techniques and analyzed via mass spectrometry (Fig. 2a). This approach was recently used to unravel the dynamics of the stress-granule proteome, as well as the compositional diversity associated with neurodegeneration-linked mutations[18]. Analogous proximity-ligation approaches have been used for interrogating the interactome in the vicinity of specific RNAs[19,20] or genomic loci[21–23]. A recent adaptation incorporating DNA barcoding has begun to yield rich insights into the way in which nuclear condensates organize chromatin architecture[24].

In addition to biochemical techniques, microscopy has been essential for gaining structural and biophysical insights into intracellular condensates, beginning with the first bright-field imaging of the nucleolus and other organelles in the 1800s and continuing through more recent developments based on advanced confocal techniques. As many condensates are sub-micron in size and therefore approach the diffraction limit of conventional fluorescence microscopy, super-resolution imaging approaches, such as stimulated emission depletion (STED)[25] microscopy, photoactivation localization microscopy (PALM)[26] and stochastic optical reconstruction microscopy (STORM)[27], are beginning to have a large impact on this field[10,28,29] and have revealed details of condensate sub-structures (Fig. 2a). For example, super-resolution microscopy of stress granules, nuclear speckles and paraspeckles have suggested underlying core-shell architectures mediated in part by RNA[29–31].

Electron microscopy techniques, such as in situ cryo-electron tomography (cryo-ET), which have recently transformed structural biology, are also beginning to have impact in the field of intracellular phase separation by allowing visualization in a label-free and environmentally unperturbed manner[32]. For example, cryo-ET was recently used to measure the pair correlation function of proteins within the pyrenoid[33], a protein body found in the chloroplasts of most eukaryotic algae, providing direct evidence for an underlying liquid-like structural organization, which contradicted the previously proposed crystalline organization. In other cases, cryo-ET has been used to measure crowding effects in biological condensates[34] and to observe the detailed structure that condensates may evolve into as they transition to irreversible, and potentially pathogenic, aggregates[35].

Material properties. Various complementary tools have been used to interrogate the material properties and associated molecular-transport dynamics within condensates (Fig. 2b). Fluorescence recovery after photobleaching (FRAP) and fluorescence loss in photobleaching (FLIP) are two extensively used approaches that take advantage of the characteristic ability of many fluorescent molecules to photobleach. In such approaches, a whole condensate or part of it is bleached, and the fluorescence signal recovery is tracked as unbleached molecules diffuse into the bleached region (Fig. 2b), providing insights into molecular mobility, differential mobility within a population and spatiotemporal changes in material state[36]. However, multiple experimental nuances, including asymmetric concentration gradient formed in half-FRAP experiments, asymmetric point-spread function, nonspherical morphology of cellular condensates and averaging over heterogenous subresolved structures, all can make diffusion-coefficient estimation a fitting-model–dependent problem[37,38].

Fluorescence correlation spectroscopy (FCS) provides a potentially more accurate means to determine molecular diffusion coefficients[4,39,40] (Fig. 2b) and can in addition be used to measure local concentration of biomolecules and the intermolecular interactions

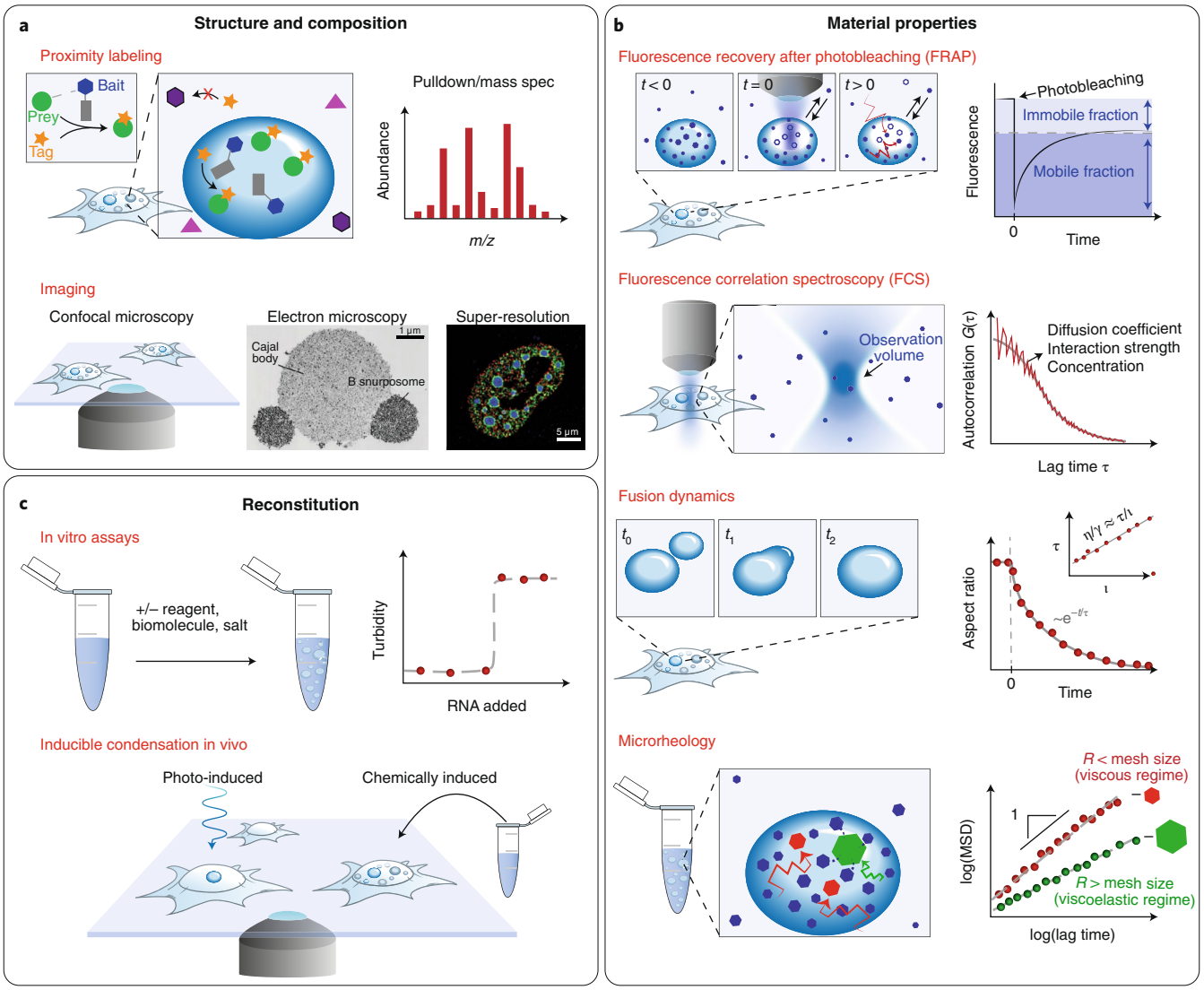

Fig. 2 | Techniques and technologies for interrogating membrane-less organelles. a, Structure and biomolecular composition can be achieved using proximity labeling approaches, which allow high-throughput identification of organelle composition, whereas advanced microscopy techniques aid in uncovering finer structural details, such as Cajal bodies seen by electron microscopy or nuclear speckles by super-resolution imaging. **b**, Material properties can be probed with imaging-based techniques, including FRAP and FCS, which elucidate condensate fluidity through molecular mobility (diffusion coefficient) and other parameters. Observation of fusion dynamics and probe particle diffusion (passive microrheology) can lead to additional inferences of material properties and state. **c**, In vitro and in vivo reconstitution can be achieved through several approaches. Single-component or reduced multicomponent systems can be used to form biomolecular droplets in controlled environments in vitro, whereas inducible systems based on optogenetics or chemical induction can be used for actuatable in vivo reconstitution. Microscopy images adapted with permission from American Society for Cell Biology[46] and The Company of Biologists, Ltd.[31].

that drive condensate formation[41,42]; nevertheless, using FCS within the dense condensate remains challenging, due to the high biomolecular concentrations in condensates and refractive index changes within cells. A complementary approach is fluorescence lifetime imaging (FLIM), which exploits an intrinsic sensitivity of fluorophores to features of their microenvironment and has recently been used to detect time-dependent changes in protein concentrations in various native condensates[43]. Although still largely underexploited to study intracellular LLPS, FLIM, as well as Förster resonance energy transfer (FRET), are powerful techniques that can be used for monitoring subsequent transitions into protein aggregative states in vivo[44,45].

The liquid-like nature of many condensates gives rise to measurable fluid properties, from classic wetting upon contact of two immiscible liquids to dripping in response to shear forces[1,46,47]; in many cases, these dynamics provide a more reliable indication of bulk material state than FRAP and other molecular mobility–based approaches. When two condensates of the same phase contact one another, they coalesce into a single larger body. The dynamics of coalescence gives rise to distinct condensate size distributions. For example, nucleoli in *Xenopus laevis* oocytes display a power-law size distribution, characteristic of a slowly coarsening emulsion[48], which spontaneously coalesces into a single large condensate when the surrounding actin matrix is disrupted[49]. The shape of two coalescing droplets exhibits exponential relaxation to a single large sphere, on a timescale dictated by the ratio of viscosity to surface tension[50] (Fig. 2b). Such dynamics have been widely used to characterize fluidity in reconstituted systems[51] as well as in live cells[48,52,53]. Using these analyses following biological perturbations can yield insights into the factors that may actively 'fluidize' native condensates[48,54].

A more direct interrogation of condensate material state can be obtained using microrheology approaches. Passive microrheology relies on tracking the Brownian motion (i.e., thermal fluctuations) of probe particles embedded within soft materials, and determining viscoelasticity using a generalized Stokes–Einstein framework[55,56] (Fig. 2b). The P-granule protein LAF-1 has been interrogated with passive microrheology[51] and was shown to exhibit an effective mesh size of 3–8 nm, which sets the length-scale threshold at which diffusion and permeability are sterically constrained by the condensate[41]. A passive microrheology approach has also been recently implemented in live cells using self-assembled tracer protein particles, revealing dramatic changes in the biophysical properties of the cytoplasm upon cellular metabolism regulation, which in turn tune biomolecular condensation[34].

A conceptually similar approach exploiting shape fluctuations has recently been used to probe the surface tension of nucleoli[52]; despite the likely importance of surface tension for many aspects of condensate function, to date only a very small number of direct measurements of surface tension have been undertaken[47]. By themselves, such passive microrheology approaches are limited by the assumption of thermal equilibrium, which may be true in some[49] but not all cases. Recently, active microrheology approaches have been used that are based on deforming reconstituted condensates using microfluidic-controlled shear stresses[57] or optically trapped particles[58], providing insights into the salt-dependent interplay between the viscosity and elasticity of condensates. Active microrheology is particularly attractive for non-equilibrium systems where thermal fluctuations may be dominated by active (for example, ATP-dependent) fluctuations, since information about the amplitude and timescales of these fluctuations can be extracted. However, such measurements are very challenging to achieve on micron length scales, particularly due to the need for disentangling the role of surface tension in the deformation response.

Building biomimetic organelles in vitro

Despite the complex composition of in vivo condensates, comparable, albeit greatly simplified, phase-separated protein droplets can be created in vitro. Assays to detect LLPS typically involve tracking of the macroscopic change in turbidity, or microscopic observation of droplet formation during perturbations of the environment of the purified protein (for example, perturbation of salt, RNA, temperature and pH; Fig. 2c)[59]. These studies have been critical for elucidating the way in which multivalency is typically achieved through a combination of (i) fluctuating IDRs with multiple self-associating patches, such as those commonly found in nucleic-acid-binding proteins[60]; (ii) protein homo- or hetero-oligomerization domains; (iii) repetitive folded interaction domains or their short binding partners, which are ubiquitous in signaling clusters[13,61–63] and (iv) nucleic acids scaffolds (Fig. 3a). Each of these can be understood as driving phase separation by decreasing the relative contribution of entropy compared to favorable interaction energy (see Box 1). These multivalent interaction modes can be regulated biologically, for example through post-translational protein modification, to amplify or suppress phase separation.

Several studies have placed particular emphasis on the importance of IDRs, which in many cases can be both necessary and sufficient for phase separation, at least when present at sufficiently high concentrations in vitro. This work includes the use of nuclear magnetic resonance (NMR) to elucidate the regulated IDR interactions and conformations that promote LLPS[64–66]. Careful study of IDR sequences has shown that they often are enriched in a subset of amino acids, and they are thus commonly referred to as low-complexity sequences. These sequences can drive IDR self-association through many classes of interactions, including dipole–dipole, ionic, cation–pi and pi–pi interactions and the hydrophobic effect[67–69] (Fig. 3a). Interestingly, amino acid patterning and spacing in the sequence, and not solely the presence of certain residues, are important determinants of phase separation[67,70]. These findings have been described in detail elsewhere[14,71].

Progress toward engineering applications has also been made with simplified models of IDRs. Elastin-like peptides (ELPs) are polypeptide repeats of the hydrophobic sequence VPGXG, where the X residue (guest residue) determines physicochemical properties[72,73]. Phase separation of ELPs is entropically driven by the free energy gain associated with the release of solvent molecules, and thereby exhibits a 'lower critical solution temperature' (LCST; i.e., phase separation upon increasing temperature) type of transition as opposed to the molecular-interaction-driven 'upper critical solution temperature' (UCST) type associated with most intracellular proteins. Interestingly, the critical transition temperature can be tuned through the selection of the guest residue composition and the number of polypeptide repeats[74,75]. A simple set of ELPs comprising only valine and alanine as the guest residue at different fractions and spacings within the polymer were able to recapitulate layered liquid droplets in vitro[72] (Fig. 4a). This is reminiscent of native condensates, such as the nucleolus, which forms a tripartite layered droplet in the nucleus (see Fig. 1)[47]. Another study extended the repetitive polypeptide framework to include differing amino acids, to develop heuristics for designing sequences with tunable LCST or UCST[76]. We are still far from being able to design sequences with the complexity of native IDRs to yield condensates with specific properties and functions, but there increasingly appears to be a clear path toward this goal.

Efforts aimed at uncovering the sequence-encoded biomolecular features driving phase separation are ongoing, but recent work has brought us to the point where we can exploit some basic principles to design synthetic organelles. For instance, repetitive chains of Src homology 3 (SH3) domains and their binding partners have been shown to form liquid-like droplets in vitro, in a manner specific to the concentration of each component[13]. Furthermore, these systems can simultaneously recruit additional proteins ('clients') containing one or more corresponding interaction domains. Such clients do not contribute to the network of interactions yielding the cluster, but instead can introduce functionality into the condensate. Notably, tunable compositional control of clients has been achieved based on the number of fused interaction domains[77]. One study applied a similar approach to IDRs: multivalent repeats of the IDR from the RNA helicase LAF-1 (RGG domain) were fused to promote phase separation in vitro, with each additional domain in the construct lowering the saturation concentration for phase separation. Client proteins tagged with tandem LAF-1 RGG domains are efficiently recruited to these condensates[78]. In vitro work with a related RNA helicase, DDX4, which is capable of phase separating, has revealed that lower-stability nucleic acid sequences (i.e., single-stranded nucleic acids with weak secondary structure) are preferentially recruited to condensates, whereas more stable structures are excluded[67,79]. Moreover, the DDX4 condensates can destabilize nucleotide duplexes[79], suggesting that local chemical properties within condensates can be engineered to achieve specific molecular processing functions.

Optogenetic and chemical actuation of in vivo condensates

In vitro studies have helped elucidate many of the fundamental biomolecular driving forces of phase separation, but it has not always been clear that the concentration and composition of in vitro mimics are physiologically relevant. Moreover, from an engineering perspective, building actuatable condensates for biomedical applications within living cells is particularly attractive (Fig. 2c). Several technologies for controlling intracellular phase separation have recently emerged, leveraging the insights gained from studies of the multivalent biomolecular interactions underlying endogenous condensates (Fig. 3a). Valence amplification, for example through

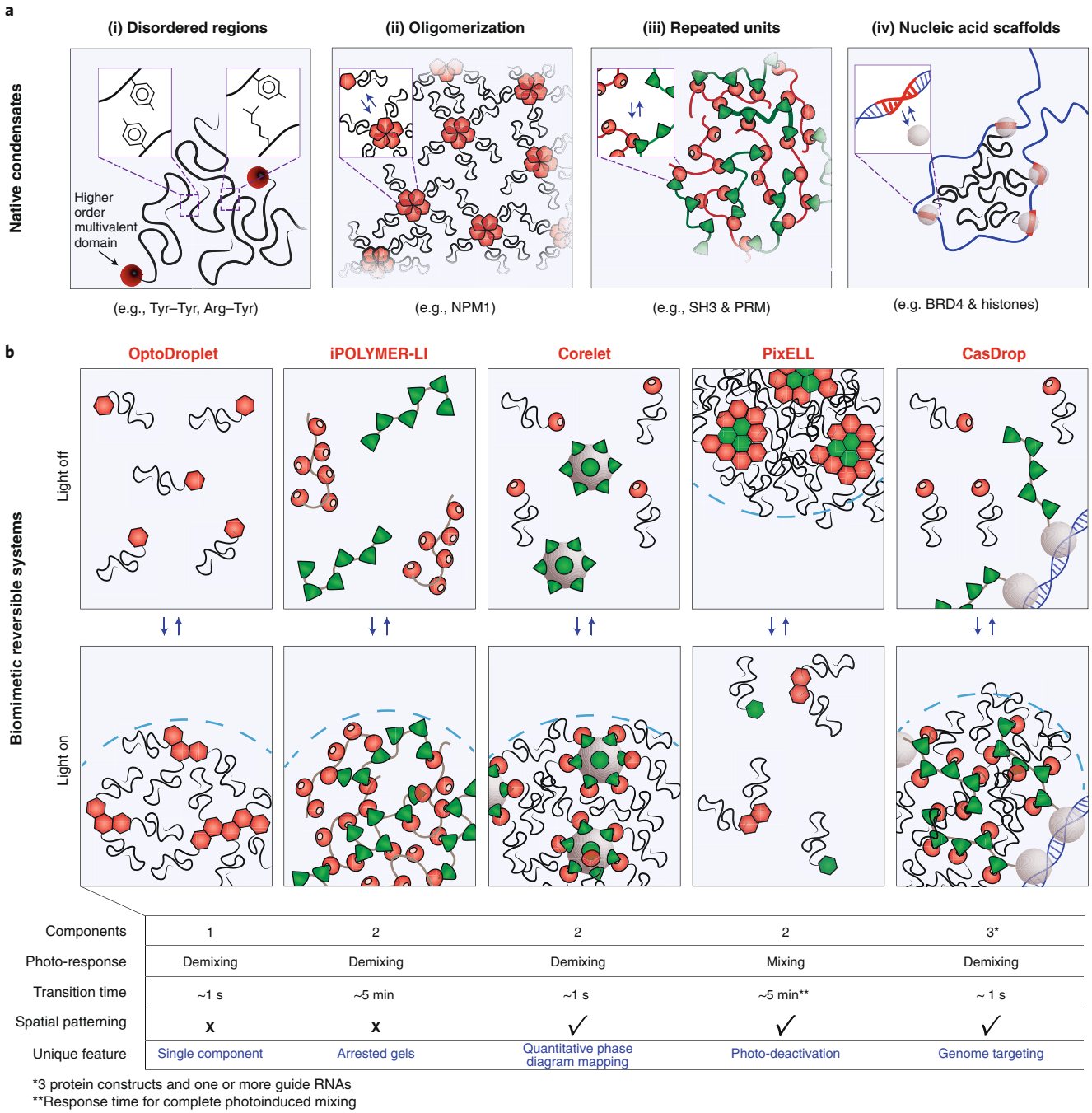

Fig. 3 | Multivalency in native and engineered condensates. a, In native condensates, multivalency is achieved in the following manner: (i) among repetitive 'sticky' residues within transiently interacting IDRs; (ii) through protein quaternary structures mediated by oligomerization domains; (iii) with repeated protein interaction domains and (iv) through scaffolding on nucleic acids via RNA recognition motifs and/or DNA-binding domains. The intrinsic multivalency of native IDRs is typically insufficient to drive intracellular LLPS at physiological protein concentrations. **b**, Currently available engineered systems that modulate multivalency using blue light to noninvasively promote or reverse intracellular LLPS (see Box 1). The degree of multivalency, which can be achieved by combining one or more of the modes shown in **a**, is directly linked to the protein concentration necessary to trigger LLPS[42].

protein-oligomerization domains, can drive phase separation by decreasing the relative importance of entropy (see Box 1), and this has been a key design concept for the nascent field of condensate engineering. Below, we discuss approaches using either light or chemicals to control oligomerization or other biomolecular interactions driving phase separation.

Light-activated phase separation. The field of optogenetics utilizes proteins whose interactions or activities depend on incident light of a particular wavelength. The first system combining optogenetic-based oligomerization with IDR-driven intracellular phase separation is called 'optoDroplet'[80] (Fig. 3b). This system takes advantage of two central features of endogenous phase-separated organelles: higher-order oligomerization and weak multivalent interactions of self-associating IDRs. IDRs from proteins known to drive phase separation in living cells were fused to Cry2, an *Arabidopsis thaliana* protein domain that forms oligomers following blue-light activation[81] (Fig. 3b). When expressed in cells, these constructs undergo

Box 1 | Thermodynamic basis for condensate engineering

Oligomerization-induced phase separation can be quantitatively described by Flory-Huggins solution polymer theory[11,109], in which a binary mixture is modeled as an infinite lattice filled with mean-field interacting solvent and solute particles. The free energy of mixing per lattice site (panel **a**) is the sum of the entropy of mixing of the solvent and solute particles, which opposes phase separation, and the particle interaction energies (enthalpy), which favors phase separation for favorable homotypic interactions designated by a positive Flory-Huggins interaction parameter χ.

The schematics in **b** display representative two-dimensional lattices describing phase separation driven by induced oligomerization from a solvent-size particle ($N = 1$) into an $N = 8$ oligomer. This results in thermodynamic instability, which is resolved by phase separation of a well-mixed solution, with a mean solute volume fraction ϕ, into two coexisting compositionally distinct phases (one dilute in solute, ϕ_A, and the other rich in solute, ϕ_B). Panel **c** displays how, mechanistically, oligomerization decreases the solute entropy of mixing, and hence reduces the overall entropic barrier for phase separation. The solvent entropy of mixing (red dashed line in **c**) remains unchanged upon solute oligomerization, representing the entropy of mixing at infinite oligomerization. The change in free energy in response to induced oligomerization (**d**) can result in phase separation, where the free energy change associated with phase separation is given by the tangent line to the free energy curve, and the composition of the dilute and dense phases is defined at the tangent points (green dots).

The two-phase coexistence regime can be described in a phase diagram as the area under the binodal coexistence line. Phase diagrams, which are often plotted as temperature (y axis) versus concentration (x axis), can also be plotted with reference to the interaction parameter χ on the y axis (**e**), which could represent how biomolecular modifications, such as protein phosphorylation or other post-translational modifications, or sequence changes can regulate LLPS. At conditions outside of binodal curve, system-wide phase separation is not possible and a single mixed phase is observed (top right cartoon). However, as the oligomerization state increases, a system may move within the binodal curve, as demonstrated with the transition from $N = 1$ to $N = 2$. Phase separation can then occur through a nucleation and growth mechanism (bottom left and rightmost cartoons) or spinodal decomposition (central cartoon), depending on the degree of supersaturation (for more information, see ref. [110]). Instead of plotting a χ-dependent phase diagram, the chain length, N, can also be shown on the y axis, as in **f**; this can be thought of as the degree of protein oligomerization, as manifested in engineered optogenetic systems[42].

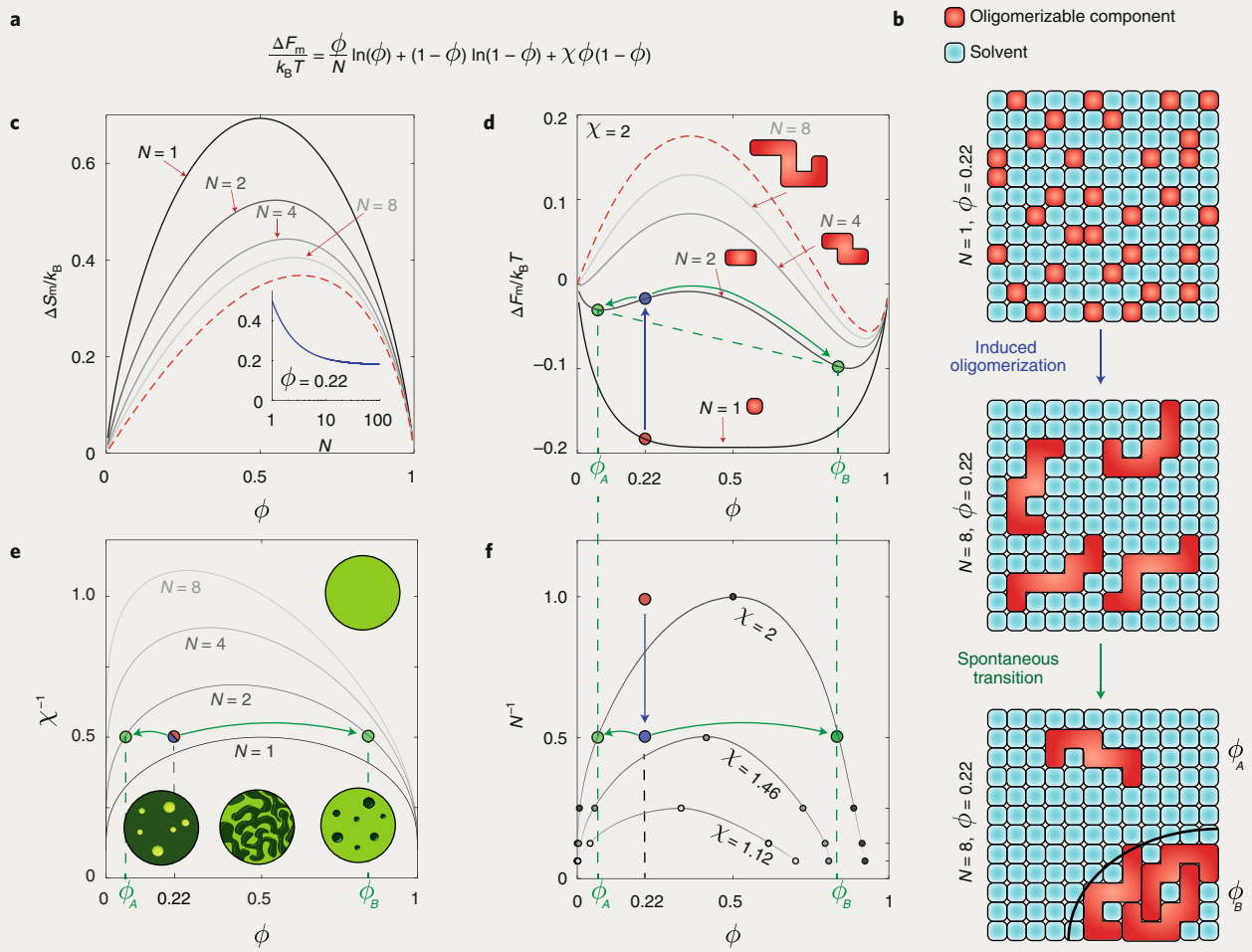

The thermodynamics of phase separation and organelle engineering. a, Equation describing the free energy of mixing, ΔF_m, where k_B is the Boltzmann constant, ϕ is the polymer/IDR volume fraction, N is the polymer/IDR chain length and χ is the Flory–Huggins interaction parameter. The first two terms represent the entropy of mixing, $\Delta S_m/k_B$, of the polymer and the solvent, respectively, and the third term is associated with the enthalpy of mixing,

Continued

Box 1 | Thermodynamic basis for condensate engineering (continued)

$\Delta H_m/k_BT$. **b**, Two-dimensional lattices describing phase separation driven by a transition from solvent-size monomer ($N = 1$) to octameric chain ($N = 8$). ϕ_A and ϕ_B designate polymer volume fraction in the dilute and dense phases, respectively. **c**, System entropy of mixing for monomer ($N = 1$) and multimers ($N = 2, 4, 8$). Red dashed line indicates the contribution of the solvent entropy of mixing to the system entropy. Inset shows the gradual decrease in the entropy of mixing at a fixed ϕ. **d**, System free energy of mixing upon oligomerization. Blue arrow shows change in free energy in response to induced dimerization (from red dot as monomer to blue dot dimer with $\chi = 2$, $N = 2$), and green arrows show how resulting phase separation (green points) lowers the free energy of the system. The red dashed line represents the free energy at maximal oligomerization, when all solute molecules are interconnected and the change in the entropy of mixing originates only in solvent molecules. Colors of arrows refer back those shown in **b**. **e**, Phase diagram of two-phase coexistence regime plotted with respect to the interaction parameter χ and as a function of volume fraction, ϕ. Red and blue dots in **d** are colocalized and represented as a half-red, half-blue dot; circles contain carton representations of phases. Colors of arrows and dots as in **d**. **f**, Phase diagram plotted with respect to the chain length, N, on the y axis with the solute volume fraction on the x axis. Colors of arrows and dots as in **d**.

LLPS in response to blue-light activation, as evident from the existence of a well-defined saturation concentration required for droplets to appear. Interestingly, a spectrum of material states could be achieved depending on the degree of supersaturation, suggesting the occurrence of a concentration-dependent gelation process that could underlie protein aggregation pathologies[80] (Fig. 4b).

The optoDroplets system is being employed in an increasing number of phase-transition studies, as a means to interrogate the role of condensates in promoting biological function or dysfunction[6,82–84]. Of particular interest is the recent use of optoDroplets to investigate the role of TDP43 in the pathogenesis of amyotrophic lateral sclerosis (ALS) and frontotemporal dementia (FTD), in which pathological phenotypes were observed in neuronal cell cultures upon extended light activation[85] (Fig. 4b). This and other recent efforts have also used the Cry2olig system, which relies on a variant of Cry2 with a point mutation that promotes potent oligomerization, leading to light-dependent aggregation/gelation behavior[86]. Fusing Cry2olig with nucleolar proteins allows light-dependent gelation of the nucleolus, which leads to ribosomal RNA (rRNA)-processing defects[87].

Despite the power of the Cry2-based systems, the oligomerization state of Cry2 is poorly defined, and Cry2–Cry2 interactions may confound the contribution of IDR to observed phase behavior. To overcome these challenges, a next-generation optogenetic system for phase separation, called Corelets, has recently been developed[42]. The Corelet system mimics the defined oligomerization of many endogenous proteins implicated in phase separation (such as the pentameric nucleolar protein Npm1), making it very powerful for quantitative interrogation of intracellular phase separation. The Corelet system uses a spherical protein core, based on the self-assembling 24-mer ferritin, in which each monomer is fused to the light-activatable protein iLID (Fig. 3b). Upon activation, iLID binds to its cognate partner (SspB), thereby recruiting any protein fused to SspB to the ferritin complex. By incorporating IDRs into these fusion proteins, Corelets are induced to phase separate into droplet condensates. The Corelet system has enabled precise quantification of the concentration and valence dependence of phase behavior, generating the first full intracellular phase diagrams, including binodal and spinodal boundaries[42] (Fig. 4c, see also Box 1 for underlying theory), within the complex cellular environment. This system has provided insights into the protein sequence dependence of the phase boundary (Fig. 4c) and revealed that the saturation concentration may be substantially decreased through nonequilibrium dynamics (i.e., local protein recruitment). A related method, PixELL, has been developed in which light is used to specifically disassemble phase-separated condensates; in the PixELL system, IDRs are fused to the PixE/PixD optogenetic proteins, which undergo oligomeric assembly in the dark and disassembly upon blue-light activation[88] (Fig. 3b).

Chemical control of phase separation. The iPOLYMER system is conceptually related to the optogenetic platforms discussed above; it is also based on the association of multivalent chains of interaction domains, which can be used to form inducible hydrogels[89]. In place of endogenous protein interaction domains, chains of FK506 binding protein (FKBP) and the FKBP-rapamycin binding protein (FRB), which associate in the presence of rapamycin, are used. Pentameric linear polymers of FKBP and FRB form clusters within minutes, and continue to grow as more FKBP and FRB protein molecules are produced by translation. An extension of this approach, iPOLYMER-LI, enables the study of reversible and light-inducible clusters formed through the association of hexameric chains of iLID and SspB[89] (Fig. 3b).

These systems have provided insights into the behavior of arsenite-induced stress granules, condensates that have biomedical importance in both neurodegeneration and viral infectivity. The RNA recognition motif of TIA-1 fused to one of the iPOLYMER chains yielded rapamycin-induced granules that colocalized with mRNA-associated proteins recruited to native stress granules[89]. However, one caveat to this and other approaches is that the synthetic structures formed may not recruit all the key stress granules proteins found in vivo, nor recapitulate the biophysical properties, organization and function of native stress granules.

Engineering condensates in and around the genome. Phase transitions within the nucleus are particularly interesting because nuclear condensates must directly interact with chromatin, and thus may potentially control its organization and gene expression. Much work has focused on the nucleolus, the largest nuclear condensate, which assembles around ribosomal DNA (rDNA) repeats. However, increasing evidence suggests that smaller nanoscale liquid-phase droplets assemble at transcriptional sites throughout the genome[6,10,90] and may even be key for heterochromatin compaction[7,8]. Although optoDroplets, Corelet and PixELL can be used in the nucleus as well as the cytoplasm, they are not designed for specifically targeting phase separation to different regions of the genome.

To address this challenge, a system termed CasDrop has been introduced. CasDrop uses an enzymatically dead dCas9 to cause phase separation at defined locations on the genome of living cells as dictated by a guide RNA[9]. CasDrop is also light activated and can be used to temporally control the assembly of condensates (Fig. 3b). Studies with this system have shown that IDRs from various nuclear proteins phase separate into liquid condensates that preferentially form in regions of low chromatin density and that mechanically exclude chromatin as they grow. These findings have led to the proposal that nuclear condensates can function as mechanoactive chromatin filters, causing distal-targeted genomic elements to be pulled together while mechanically excluding non-specific background components of the genome (Fig. 4d). Given the apparent nucleic acid melting capacity of IDR-containing proteins such as DDX4, IDRs could play a role in enhancing the accessibility of DNA at sites of transcription, or could potentially

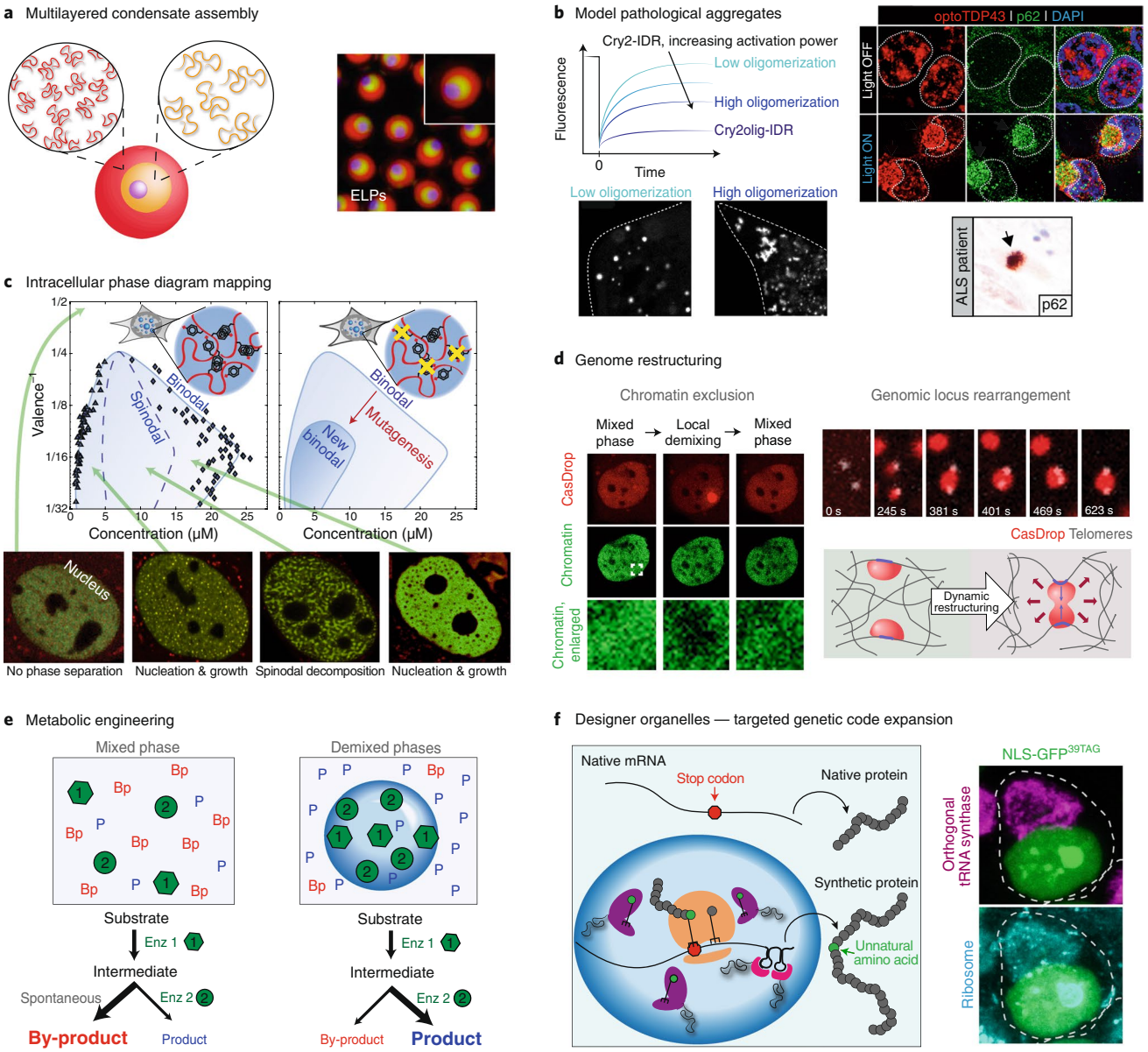

Fig. 4 | Applications of engineered condensates. a, Elastin-like peptides can be engineered to form layered structures. **b**, OptoDroplets show decreasing fluidity as a result of higher oligomerization through increased activation power or when the Cry2olig variant is used. This effect has been used to form light-inducible model pathogenic aggregates that are positive for common ALS markers, such as p62. **c**, Quantitative intracellular phase diagrams can be mapped with the Corelet system that show classic modes of formation (i.e., spinodal decomposition versus nucleation and growth). The phase diagram is sensitive to mutagenesis of the IDR, such as the removal of a subset of the tyrosine residues. **d**, CasDrop reveals that nuclear condensates interact with the genome through exclusion of chromatin and rearrangement of telomeres by dCas9-mediated localization of condensates to these sites. **e**, Enzymes recruited to engineered condensates can enhance the flux of an intermediate to the desired product over the spontaneous formation of a by-product. **f**, Engineered 'orthogonally translating' organelles yield specific genetic code expansion with minimal effect on native transcripts. These organelles are visualized by staining for the orthogonal tRNA synthase in tissue culture cells expressing a nuclear-localized green fluorescent protein (GFP) transcript with an internal stop codon (NLS-GFP^{39TAG} codon, corresponding to the orthogonal tRNA). Components not specifically tagged for recruitment yet essential for translation, such as ribosomes, are able to partition into these membrane-less organelles. Microscopy images adapted or reproduced with permission from Springer Nature Limited[72], Elsevier[9,42,80,85] and AAAS[102].

be used to engineer protocell systems[91–93] in which cycles of DNA melting could facilitate replication.

Another set of promising approaches allows the engineering of genomic interactions with phase-separated bodies. For example, the CRISPR-GO system causes particular genomic loci to interact with native nuclear bodies[94]. Recruitment of such loci to Cajal bodies leads to long-range transcriptional repression at distal loci up to 575 kb from the recruited site. Another system, called light-activated dynamic looping (LADL), takes advantage of Cry2 to drive local genomic rearrangements through engineered looping interactions[95]. In combination with recent approaches, such as split-pool recognition of interactions by tag extension (SPRITE)[24], to probe genomic organization in relation to native condensates, these tools will enable a high degree of programmability when engineering condensate behavior and reading out the corresponding structural and functional consequences for the genome.

Controlling intracellular biochemistry with synthetic condensates

Colocalizing the enzymes of a particular pathway is a common cellular mechanism for enhancing metabolic efficiency. Many membrane-bound organelles are used for this purpose, including mitochondria in the case of cellular respiration or the peroxisome for β-oxidation of fatty acids. Likewise, pathways engineered to localize into particular organelles enhance product titer through mitigation of intermediate loss to competing pathways and sequestration of toxic intermediates[96]. Even without membranes, condensates can contribute a similar means of intermediate channeling to enhance product yield from recruited pathways[97]. For example, purinosomes dynamically form in tissue culture cells deprived of purine precursors and are enriched in the enzymes that constitute the de novo purine biosynthesis pathway[98].

Enzyme recruitment to synthetic organelles can induce preferential carbon flux through a branched metabolic pathway. OptoDroplet- and PixELL-based organelles have been functionalized with a two-enzyme pathway that catalyzes the formation of a product through an intermediate which is spontaneously and non-enzymatically oxidized to a by-product. Fusion of these enzymes to the clustering components leads to enhanced product biosynthesis when condensate formation is induced in either optogenetic system[99] (Fig. 4e). Although this is promising proof-of-principle evidence supporting the adoption of synthetic condensates for metabolic engineering, the research has also encountered shortcomings that need to be addressed in order for this approach to be robustly applied to pathways of interest: fusion of large clustering tags to enzymes can reduce enzyme activity, and some enzyme fusions lead to constitutive clusters that defeat the benefits of light control[99].

The ability of condensate organelles to behave as reaction crucibles is not limited to metabolic pathways. Biomimetic dextran droplets have been shown to drive >1,000-fold RNA enrichment that can enhance the kinetics of ribozyme cleavage of substrate RNA by 50-fold as compared with a diffuse control[92]. Moreover, microtubule growth is increasingly viewed as linked to condensate nucleation, with key steps having been reconstituted in vitro, including the liquid-like centrosome's ability to enrich tubulin and nucleate microtubule asters[100]. Reconstituted signaling condensates can nucleate actin filaments important for the T cell response[101], which could suggest approaches for immune therapies based on creating synthetic condensates. Progress toward engineered signaling condensates has also been made with membrane-bound optoDroplets that cause light-activatable clustering of the receptor tyrosine kinase of fibroblast growth factor receptor (FGFR), wherein cross-phosphorylation leads to a measurable increase in ERK signaling and cell migration[88].

Finally, novel functionalities can be incorporated into engineered condensates that take advantage of their unique attributes. A striking example is 'orthogonally translating' organelles, which offer a new approach to genetic code expansion that reduces off-target utilization in native proteins[102]. Typically, genetic code expansion is achieved with tRNA–tRNA synthase pairs that introduce unnatural amino acids in place of a stop codon. The amber stop codon is often targeted for suppression as it is used in fewer than 10% of genes in *Escherichia coli*. This is more problematic in human cell lines, in which the amber stop codon is used in ~20% of the genome, so that the resulting suppression could yield substantial off-target effects. To mitigate this problem, mRNAs targeted for stop codon suppression and the unnatural tRNA synthase can be coenriched into condensates engineered with IDR tags (Fig. 4f). Notably, highly specific stop codon suppression is only achieved when the components are also localized to microtubule ends, potentially allowing effective condensate nucleation by inducing IDR multivalency[102]. A condensate organelle is arguably critical for this function, as it allows partitioning of the numerous components necessary for translation as well as endoplasmic reticulum accessibility for the translation of membrane-bound proteins with noncanonical amino acids.

Outlook

Methods inspired by engineering and physics have had an increasingly large impact on elucidating the biophysical driving forces underlying intracellular condensates. Burgeoning knowledge about these structures has advanced to the point where we can not only understand but also manipulate endogenous condensates and even engineer completely novel structures.

Accounting for and controlling the thermodynamics underlying the way these structures form will be a critical for future engineering efforts (see Box 1). For example, tuning oligomerization in a localized region of the cell can lead to global changes in the entropy of mixing by creating site-specific 'entropic sinks' that allow phase separation, even at low protein abundance[42]. Alternatively, perturbing biomolecule interaction energy, either through manipulation of IDRs or through multiple folded interaction domains (for example, post-translational modifications or mutagenesis), can likewise modulate phase separation[42,65]. Techniques such as those described in Fig. 3b, particularly those using rapid and reversible optogenetic control, can successfully drive condensate assembly and disassembly at spatiotemporally definable locations in the cell. These approaches have yielded several examples of condensate engineering, from control of genomic organization and function to metabolic flux enhancement and design of bio-orthogonal protein translation compartments. Together with our increasing understanding of the principles underlying multiphase condensates[47,72], these studies provide a foundation for engineering even more complex functions into living cells.

As has been the case in the fields of tissue engineering and synthetic biology, progress in the condensate field is emerging from a close interplay between basic science and engineering. We can now envision applications ranging from drug-delivery platforms[103] to therapeutic approaches[104] targeting diverse condensates associated with oncogenic transformation or those underlying ALS, Alzheimer's and various other protein-aggregation diseases. Future studies will continue to build on ongoing fundamental studies and define new engineering modes that interface with endogenous biological structures, from the cytoskeleton to the endomembrane system and beyond. Phase transitions reflect an underlying collective biomolecular organization, and our ability to harness this fundamental self-assembly principle for engineering applications is the basis for the emerging new field of condensate engineering.

Reporting Summary. Further information on research design is available in the Nature Research Reporting Summary linked to this article.

Received: 11 June 2019; Accepted: 28 October 2019;
Published online: 2 December 2019

References

1. Brangwynne, C. P. et al. Germline P granules are liquid droplets that localize by controlled dissolution/condensation. *Science* **324**, 1729–1732 (2009).
2. Shin, Y. & Brangwynne, C. P. Liquid phase condensation in cell physiology and disease. *Science* **357**, eaaf4382 (2017).
3. Banani, S. F., Lee, H. O., Hyman, A. A. & Rosen, M. K. Biomolecular condensates: organizers of cellular biochemistry. *Nat. Rev. Mol. Cell Biol.* **18**, 285–298 (2017).
4. Berry, J., Weber, S. C., Vaidya, N., Haataja, M. & Brangwynne, C. P. RNA transcription modulates phase transition-driven nuclear body assembly. *Proc. Natl Acad. Sci. USA* **112**, E5237–E5245 (2015).
5. Molliex, A. et al. Phase separation by low complexity domains promotes stress granule assembly and drives pathological fibrillization. *Cell* **163**, 123–133 (2015).
6. Sabari, B. R. et al. Coactivator condensation at super-enhancers links phase separation and gene control. *Science* **361**, eaar3958 (2018).

7. Strom, A. R. et al. Phase separation drives heterochromatin domain formation. *Nature* **547**, 241–245 (2017).
8. Larson, A. G. et al. Liquid droplet formation by HP1α suggests a role for phase separation in heterochromatin. *Nature* **547**, 236–240 (2017).
9. Shin, Y. et al. Liquid nuclear condensates mechanically sense and restructure the genome. *Cell* **175**, 1481–1491.e13 (2018).
10. Cho, W.-K. et al. Mediator and RNA polymerase II clusters associate in transcription-dependent condensates. *Science* **361**, 412–415 (2018).
11. Flory, P. J. *Principles of Polymer Chemistry* (Cornell University Press, 1953).
12. Rubinstein, M. & Colby, R. H. *Polymer Physics* (Oxford University Press, 2003).
13. Li, P. et al. Phase transitions in the assembly of multivalent signalling proteins. *Nature* **483**, 336–340 (2012).
14. Brangwynne, C. P., Tompa, P. & Pappu, R. V. Polymer physics of intracellular phase transitions. *Nat. Phys.* **11**, 899–904 (2015).
15. Putnam, A., Cassani, M., Smith, J. & Seydoux, G. A gel phase promotes condensation of liquid P granules in *Caenorhabditis elegans* embryos. *Nat. Struct. Mol. Biol.* **26**, 220–226 (2019).
16. Roux, K. J., Kim, D. I., Raida, M. & Burke, B. A promiscuous biotin ligase fusion protein identifies proximal and interacting proteins in mammalian cells. *J. Cell Biol.* **196**, 801–810 (2012).
17. Rhee, H. W. et al. Proteomic mapping of mitochondria in living cells via spatially restricted enzymatic tagging. *Science* **339**, 1328–1331 (2013).
18. Markmiller, S. et al. Context-dependent and disease-specific diversity in protein interactions within stress granules. *Cell* **172**, 590–604.e13 (2018).
19. Ramanathan, M. et al. RNA-protein interaction detection in living cells. *Nat. Methods* **15**, 207–212 (2018).
20. Huang, R., Han, M., Meng, L. & Chen, X. Transcriptome-wide discovery of coding and noncoding RNA-binding proteins. *Proc. Natl Acad. Sci. USA* **115**, E3879–E3887 (2018).
21. Schmidtmann, E., Anton, T., Rombaut, P., Herzog, F. & Leonhardt, H. Determination of local chromatin composition by CasID. *Nucleus* **7**, 476–484 (2016).
22. Myers, S. A. et al. Discovery of proteins associated with a predefined genomic locus via dCas9-APEX-mediated proximity labeling. *Nat. Methods* **15**, 437–439 (2018).
23. Gao, X. D. et al. C-BERST: defining subnuclear proteomic landscapes at genomic elements with dCas9-APEX2. *Nat. Methods* **15**, 433–436 (2018).
24. Quinodoz, S. A. et al. Higher-order inter-chromosomal hubs shape 3D genome organization in the nucleus. *Cell* **174**, 744–757.e24 (2018).
25. Klar, T. A., Jakobs, S., Dyba, M., Egner, A. & Hell, S. W. Fluorescence microscopy with diffraction resolution barrier broken by stimulated emission. *Proc. Natl Acad. Sci. USA* **97**, 8206–8210 (2000).
26. Betzig, E. et al. Imaging intracellular fluorescent proteins at nanometer resolution. *Science* **313**, 1642–1645 (2006).
27. Rust, M. J., Bates, M. & Zhuang, X. Sub-diffraction-limit imaging by stochastic optical reconstruction microscopy (STORM). *Nat. Methods* **3**, 793–795 (2006).
28. Wang, J. T. et al. Regulation of RNA granule dynamics by phosphorylation of serine-rich, intrinsically disordered proteins in *C. elegans*. *eLife* **3**, e04591 (2014).
29. Jain, S. et al. ATPase-modulated stress granules contain a diverse proteome and substructure. *Cell* **164**, 487–498 (2016).
30. West, J. A. et al. Structural, super-resolution microscopy analysis of paraspeckle nuclear body organization. *J. Cell Biol.* **214**, 817–830 (2016).
31. Fei, J. et al. Quantitative analysis of multilayer organization of proteins and RNA in nuclear speckles at super resolution. *J. Cell. Sci.* **130**, 4180–4192 (2017).
32. Asano, S., Engel, B. D. & Baumeister, W. In situ cryo-electron tomography: a post-reductionist approach to structural biology. *J. Mol. Biol.* **428**, 332–343 (2016). 2 Pt A.
33. Freeman Rosenzweig, E. S. et al. The eukaryotic CO_2-concentrating organelle is liquid-like and exhibits dynamic reorganization. *Cell* **171**, 148–162.e19 (2017).
34. Delarue, M. et al. mTORC1 controls phase separation and the biophysical properties of the cytoplasm by tuning crowding. *Cell* **174**, 338–349.e20 (2018).
35. Guo, Q. et al. In Situ Structure of Neuronal C9orf72 Poly-GA Aggregates Reveals Proteasome Recruitment. *Cell* **172**, 696–705.e12 (2018).
36. Ishikawa-Ankerhold, H. C., Ankerhold, R. & Drummen, G. P. C. Advanced fluorescence microscopy techniques—FRAP, FLIP, FLAP, FRET and FLIM. *Molecules* **17**, 4047–4132 (2012).
37. Mueller, F., Mazza, D., Stasevich, T. J. & McNally, J. G. FRAP and kinetic modeling in the analysis of nuclear protein dynamics: what do we really know? *Curr. Opin. Cell Biol.* **22**, 403–411 (2010).
38. Taylor, N. O., Wei, M., Stone, H. A. & Brangwynne, C. P. Quantifying phase-separated protein condensates using fluorescence recovery after photobleaching. *Biophys. J.* **117**, 1285–1300 (2019).
39. Weidtkamp-Peters, S. et al. Dynamics of component exchange at PML nuclear bodies. *J. Cell Sci.* **121**, 2731–2743 (2008).
40. Magde, D., Elson, E. & Webb, W. W. Thermodynamic fluctuations in a reacting system—measurement by fluorescence correlation spectroscopy. *Phys. Rev. Lett.* **29**, 705–708 (1972).
41. Wei, M.-T. et al. Phase behaviour of disordered proteins underlying low density and high permeability of liquid organelles. *Nat. Chem.* **9**, 1118–1125 (2017).
42. Bracha, D. et al. Mapping local and global liquid phase behavior in living cells using photo-oligomerizable seeds. *Cell* **175**, 1467–1480.e13 (2018).
43. Pliss, A. et al. Cycles of protein condensation and discharge in nuclear organelles studied by fluorescence lifetime imaging. *Nat. Commun.* **10**, 455 (2019).
44. Kaminski Schierle, G. S. et al. A FRET sensor for non-invasive imaging of amyloid formation in vivo. *ChemPhysChem* **12**, 673–680 (2011).
45. Laine, R. F. et al. Fast fluorescence lifetime imaging reveals the aggregation processes of α-synuclein and polyglutamine in aging *Caenorhabditis elegans*. *ACS Chem. Biol.* **14**, 1628–1636 (2019).
46. Gall, J. G., Bellini, M., Wu, Z. & Murphy, C. Assembly of the nuclear transcription and processing machinery: Cajal bodies (coiled bodies) and transcriptosomes. *Mol. Biol. Cell* **10**, 4385–4402 (1999).
47. Feric, M. et al. Coexisting liquid phases underlie nucleolar subcompartments. *Cell* **165**, 1686–1697 (2016).
48. Brangwynne, C. P., Mitchison, T. J. & Hyman, A. A. Active liquid-like behavior of nucleoli determines their size and shape in *Xenopus laevis* oocytes. *Proc. Natl Acad. Sci. USA* **108**, 4334–4339 (2011).
49. Feric, M. & Brangwynne, C. P. A nuclear F-actin scaffold stabilizes ribonucleoprotein droplets against gravity in large cells. *Nat. Cell Biol.* **15**, 1253–1259 (2013).
50. Eggers, J., Lister, J. R. & Stone, H. A. Coalescence of liquid drops. *J. Fluid Mech.* **401**, 293–310 (1999).
51. Elbaum-Garfinkle, S. et al. The disordered P granule protein LAF-1 drives phase separation into droplets with tunable viscosity and dynamics. *Proc. Natl Acad. Sci. USA* **112**, 7189–7194 (2015).
52. Caragine, C. M., Haley, S. C. & Zidovska, A. Surface fluctuations and coalescence of nucleolar droplets in the human cell nucleus. *Phys. Rev. Lett.* **121**, 148101 (2018).
53. Hubstenberger, A., Noble, S. L., Cameron, C. & Evans, T. C. Translation repressors, an RNA helicase, and developmental cues control RNP phase transitions during early development. *Dev. Cell* **27**, 161–173 (2013).
54. Patel, A. et al. ATP as a biological hydrotrope. *Science* **356**, 753–756 (2017).
55. Wirtz, D. Particle-tracking microrheology of living cells: principles and applications. *Annu. Rev. Biophys.* **38**, 301–326 (2009).
56. Mason, T. G. & Weitz, D. A. Optical measurements of frequency-dependent linear viscoelastic moduli of complex fluids. *Phys. Rev. Lett.* **74**, 1250–1253 (1995).
57. Taylor, N. et al. Biophysical characterization of organelle-based RNA/protein liquid phases using microfluidics. *Soft Matter* **12**, 9142–9150 (2016).
58. Jawerth, L. M. et al. Salt-dependent rheology and surface tension of protein condensates using optical traps. *Phys. Rev. Lett.* **121**, 258101 (2018).
59. Alberti, S., Gladfelter, A. & Mittag, T. Considerations and challenges in studying liquid-liquid phase separation and biomolecular condensates. *Cell* **176**, 419–434 (2019).
60. Castello, A. et al. Insights into RNA biology from an atlas of mammalian mRNA-binding proteins. *Cell* **149**, 1393–1406 (2012).
61. Pawson, T. & Nash, P. Assembly of cell regulatory systems through protein interaction domains. *Science* **300**, 445–452 (2003).
62. Cohen, G. B., Ren, R. & Baltimore, D. Modular binding domains in signal transduction proteins. *Cell* **80**, 237–248 (1995).
63. Schwarz-Romond, T., Merrifield, C., Nichols, B. J. & Bienz, M. The Wnt signalling effector Dishevelled forms dynamic protein assemblies rather than stable associations with cytoplasmic vesicles. *J. Cell Sci.* **118**, 5269–5277 (2005).
64. Burke, K. A., Janke, A. M., Rhine, C. L. & Fawzi, N. L. Residue-by-residue view of in vitro FUS granules that bind the C-terminal domain of RNA polymerase II.
65. Monahan, Z. et al. Phosphorylation of the FUS low-complexity domain disrupts phase separation, aggregation, and toxicity. *EMBO J.* **36**, 2951–2967 (2017).
66. Brady, J. P. et al. Structural and hydrodynamic properties of an intrinsically disordered region of a germ cell-specific protein on phase separation. *Proc. Natl Acad. Sci. USA* **114**, E8194–E8203 (2017).
67. Nott, T. J. et al. Phase transition of a disordered nuage protein generates environmentally responsive membraneless organelles. *Mol. Cell* **57**, 936–947 (2015).
68. Wang, J. et al. A Molecular grammar governing the driving forces for phase separation of prion-like RNA binding proteins. *Cell* **174**, 688–699.e16 (2018).

69. Riback, J. A. et al. Stress-triggered phase separation is an adaptive, evolutionarily tuned response. *Cell* **168**, 1028–1040.e19 (2017).
70. Das, R. K. & Pappu, R. V. Conformations of intrinsically disordered proteins are influenced by linear sequence distributions of oppositely charged residues. *Proc. Natl Acad. Sci. USA* **110**, 13392–13397 (2013).
71. Martin, E. W. & Mittag, T. Relationship of sequence and phase separation in protein low-complexity regions. *Biochemistry* **57**, 2478–2487 (2018).
72. Simon, J. R., Carroll, N. J., Rubinstein, M., Chilkoti, A. & López, G. P. Programming molecular self-assembly of intrinsically disordered proteins containing sequences of low complexity. *Nat. Chem.* **9**, 509–515 (2017).
73. Roberts, S., Dzuricky, M. & Chilkoti, A. Elastin-like polypeptides as models of intrinsically disordered proteins. *FEBS Lett.* **589**, 2477–2486 (2015). 19 Pt A.
74. Urry, D. W. Physical chemistry of biological free energy transduction as demonstrated by elastic protein-based polymers †. *J. Phys. Chem. B* **101**, 11007–11028 (1997).
75. Urry, D. W. The change in Gibbs free energy for hydrophobic association: Derivation and evaluation by means of inverse temperature transitions. *Chem. Phys. Lett.* **399**, 177–183 (2004).
76. Quiroz, F. G. & Chilkoti, A. Sequence heuristics to encode phase behaviour in intrinsically disordered protein polymers. *Nat. Mater.* **14**, 1164–1171 (2015).
77. Banani, S. F. et al. Compositional control of phase-separated cellular bodies. *Cell* **166**, 651–663 (2016).
78. Schuster, B. S. et al. Controllable protein phase separation and modular recruitment to form responsive membraneless organelles. *Nat. Commun.* **9**, 2985 (2018).
79. Nott, T. J., Craggs, T. D. & Baldwin, A. J. Membraneless organelles can melt nucleic acid duplexes and act as biomolecular filters. *Nat. Chem.* **8**, 569–575 (2016).
80. Shin, Y. et al. Spatiotemporal control of intracellular phase transitions using light-activated optoDroplets. *Cell* **168**, 159–171.e14 (2017).
81. Más, P., Devlin, P. F., Panda, S. & Kay, S. A. Functional interaction of phytochrome B and cryptochrome 2. *Nature* **408**, 207–211 (2000).
82. Zhang, P. et al. Chronic optogenetic induction of stress granules is cytotoxic and reveals the evolution of ALS-FTD pathology. *eLife* **8**, e39578 (2019).
83. Wei, M.-T., Chang, Y.-C., Shimobayashi, S. F., Shin, Y. & Brangwynne, C. P. Nucleated transcriptional condensates amplify gene expression. Preprint at https://www.biorxiv.org/content/10.1101/737387 (2019).
84. Liao, Y.-C. et al. RNA granules hitchhike on lysosomes for long-distance transport, using annexin A11 as a molecular tether. *SSRN Electron. J.* https://doi.org/10.2139/ssrn.3312723 (2019).
85. Mann, J. R. et al. RNA binding antagonizes neurotoxic phase transitions of TDP-43. *Neuron* **102**, 321–338.e8 (2019).
86. Taslimi, A. et al. An optimized optogenetic clustering tool for probing protein interaction and function. *Nat. Commun.* **5**, 4925 (2014).
87. Zhu, L. et al. Controlling the material properties and rRNA processing function of the nucleolus using light. *Proc. Natl Acad. Sci. USA* **116**, 17330–17335 (2019).
88. Dine, E., Gil, A. A., Uribe, G., Brangwynne, C. P. & Toettcher, J. E. Protein phase separation provides long-term memory of transient spatial stimuli. *Cell Syst.* **6**, 655–663.e5 (2018).
89. Nakamura, H. et al. Intracellular production of hydrogels and synthetic RNA granules by multivalent molecular interactions. *Nat. Mater.* **17**, 79–89 (2018).
90. Chong, S. et al. Imaging dynamic and selective low-complexity domain interactions that control gene transcription. *Science* **361**, eaar2555 (2018).
91. Zwicker, D., Seyboldt, R., Weber, C. A., Hyman, A. A. & Jülicher, F. Growth and division of active droplets provides a model for protocells. *Nat. Phys.* **13**, 408–413 (2017).
92. Strulson, C. A., Molden, R. C., Keating, C. D. & Bevilacqua, P. C. RNA catalysis through compartmentalization. *Nat. Chem.* **4**, 941–946 (2012).
93. Drobot, B. et al. Compartmentalised RNA catalysis in membrane-free coacervate protocells. *Nat. Commun.* **9**, 3643 (2018).
94. Wang, H. et al. CRISPR-mediated programmable 3D genome positioning and nuclear organization. *Cell* **175**, 1405–1417.e14 (2018).
95. Rege, M. et al. LADL: light-activated dynamic looping for endogenous gene expression control. Preprint at https://www.biorxiv.org/content/10.1101/349340 (2018).
96. Hammer, S. K. & Avalos, J. L. Harnessing yeast organelles for metabolic engineering. *Nat. Chem. Biol.* **13**, 823–832 (2017).
97. Castellana, M. et al. Enzyme clustering accelerates processing of intermediates through metabolic channeling. *Nat. Biotechnol.* **32**, 1011–1018 (2014).
98. An, S., Kumar, R., Sheets, E. D. & Benkovic, S. J. Reversible compartmentalization of de novo purine biosynthetic complexes in living cells. *Science* **320**, 103–106 (2008).
99. Zhao, E. M. et al. Light-based control of metabolic flux through assembly of synthetic organelles. *Nat. Chem. Biol.* **15**, 589–597 (2019).
100. Woodruff, J. B. et al. The centrosome is a selective condensate that nucleates microtubules by concentrating tubulin. *Cell* **169**, 1066–1077.e10 (2017).
101. Su, X. et al. Phase separation of signaling molecules promotes T cell receptor signal transduction. *Science* **352**, 595–599 (2016).
102. Reinkemeier, C. D., Girona, G. E. & Lemke, E. A. Designer membraneless organelles enable codon reassignment of selected mRNAs in eukaryotes. *Science* **363**, eaaw2644 (2019).
103. McDaniel, J. R., Callahan, D. J. & Chilkoti, A. Drug delivery to solid tumors by elastin-like polypeptides. *Adv. Drug Deliv. Rev.* **62**, 1456–1467 (2010).
104. Mullard, A. Biomolecular condensates pique drug discovery curiosity. *Nat. Rev. Drug Discov.* https://doi.org/10.1038/d41573-019-00069-w (2019).
105. Case, L. B., Zhang, X., Ditlev, J. A. & Rosen, M. K. Stoichiometry controls activity of phase-separated clusters of actin signaling proteins. *Science* **363**, 1093–1097 (2019).
106. Boke, E. et al. Amyloid-like self-assembly of a cellular compartment. *Cell* **166**, 637–650 (2016).
107. Mateju, D. et al. An aberrant phase transition of stress granules triggered by misfolded protein and prevented by chaperone function. *EMBO J.* **36**, 1669–1687 (2017).
108. Jastrow, H. *Dr. Jastrow's Electron Microscopic Atlas* http://www.drjastrow.de/WAI/EM/EMAtlas.html (accessed 23 October 2019).
109. Rubinstein, M. & Colby, R. H. *Polymer Physics* (Oxford University Press, 2003).
110. Berry, J., Brangwynne, C. P. & Haataja, M. Physical principles of intracellular organization via active and passive phase transitions. *Rep. Prog. Phys.* **81**, 046601 (2018).

Acknowledgements

We thank members of the Brangwynne laboratory for comments on the manuscript. This work was supported by the Howard Hughes Medical Institute and by grants from the NIH 4D Nucleome Program (U01 DA040601), the Princeton Center for Complex Materials, and an NSF-supported MRSEC (DMR 1420541). D.B. acknowledges support through a Cross-Disciplinary Postdoctoral Fellowship from the Human Frontiers Science Program. M.T.W. is supported by the National Science Foundation Graduate Research Fellowship Program under grant no. DGE-1656466.

Competing interests

The authors have filed patents on technologies discussed, including the Corelet, CasDrop and optoDroplet systems.

Additional information

Supplementary information is available for this paper at https://doi.org/10.1038/s41587-019-0341-6.

Correspondence should be addressed to C.P.B.

Reprints and permissions information is available at www.nature.com/reprints.

Publisher's note Springer Nature remains neutral with regard to jurisdictional claims in published maps and institutional affiliations.

nature research

Corresponding author(s): Clifford P. Brangwynne

Last updated by author(s): Sep 4, 2019

Reporting Summary

Nature Research wishes to improve the reproducibility of the work that we publish. This form provides structure for consistency and transparency in reporting. For further information on Nature Research policies, see Authors & Referees and the Editorial Policy Checklist.

Statistics

For all statistical analyses, confirm that the following items are present in the figure legend, table legend, main text, or Methods section.

n/a	Confirmed	
☒	☐	The exact sample size (*n*) for each experimental group/condition, given as a discrete number and unit of measurement
☒	☐	A statement on whether measurements were taken from distinct samples or whether the same sample was measured repeatedly
☒	☐	The statistical test(s) used AND whether they are one- or two-sided *Only common tests should be described solely by name; describe more complex techniques in the Methods section.*
☒	☐	A description of all covariates tested
☒	☐	A description of any assumptions or corrections, such as tests of normality and adjustment for multiple comparisons
☒	☐	A full description of the statistical parameters including central tendency (e.g. means) or other basic estimates (e.g. regression coefficient) AND variation (e.g. standard deviation) or associated estimates of uncertainty (e.g. confidence intervals)
☒	☐	For null hypothesis testing, the test statistic (e.g. *F*, *t*, *r*) with confidence intervals, effect sizes, degrees of freedom and *P* value noted *Give P values as exact values whenever suitable.*
☒	☐	For Bayesian analysis, information on the choice of priors and Markov chain Monte Carlo settings
☒	☐	For hierarchical and complex designs, identification of the appropriate level for tests and full reporting of outcomes
☒	☐	Estimates of effect sizes (e.g. Cohen's *d*, Pearson's *r*), indicating how they were calculated

Our web collection on statistics for biologists contains articles on many of the points above.

Software and code

Policy information about availability of computer code

Data collection	no data collected
Data analysis	Theory for "Box" was plotted with Matlab R2017b

For manuscripts utilizing custom algorithms or software that are central to the research but not yet described in published literature, software must be made available to editors/reviewers. We strongly encourage code deposition in a community repository (e.g. GitHub). See the Nature Research guidelines for submitting code & software for further information.

Data

Policy information about availability of data

All manuscripts must include a data availability statement. This statement should provide the following information, where applicable:

- Accession codes, unique identifiers, or web links for publicly available datasets
- A list of figures that have associated raw data
- A description of any restrictions on data availability

The data generated to support the "Box" are available from the corresponding author upon reasonable request.

Field-specific reporting

Please select the one below that is the best fit for your research. If you are not sure, read the appropriate sections before making your selection.

☒ Life sciences ☐ Behavioural & social sciences ☐ Ecological, evolutionary & environmental sciences

For a reference copy of the document with all sections, see nature.com/documents/nr-reporting-summary-flat.pdf

Life sciences study design

All studies must disclose on these points even when the disclosure is negative.

Sample size	No studies performed
Data exclusions	No studies performed
Replication	No studies performed
Randomization	No studies performed
Blinding	No studies performed

Reporting for specific materials, systems and methods

We require information from authors about some types of materials, experimental systems and methods used in many studies. Here, indicate whether each material, system or method listed is relevant to your study. If you are not sure if a list item applies to your research, read the appropriate section before selecting a response.

Materials & experimental systems

n/a	Involved in the study
☒	☐ Antibodies
☒	☐ Eukaryotic cell lines
☒	☐ Palaeontology
☒	☐ Animals and other organisms
☒	☐ Human research participants
☒	☐ Clinical data

Methods

n/a	Involved in the study
☒	☐ ChIP-seq
☒	☐ Flow cytometry
☒	☐ MRI-based neuroimaging